Title

A model for traumatic brain injury using laser induced shockwaves

ISBN

9781628417142

Authors

Selfridge, A

Preece, D

Gomez, V

et al.

Publication Date

2015-08-25

DOI

10.1117/12.2189724

PROCEEDINGS OF SPIE

SPIEDigitalLibrary.org/conference-proceedings-of-spie

A model for traumatic brain injury using laser induced shockwaves

A. Selfridge, D. Preece, V. Gomez, L. Shi, M. Berns

A. Selfridge, D. Preece, V. Gomez, L. Z. Shi, M. W. Berns, "A model for traumatic brain injury using laser induced shockwaves," Proc. SPIE 9548, Optical Trapping and Optical Micromanipulation XII, 95480P (25 August 2015); doi: 10.1117/12.2189724

SPIE.

Event: SPIE Nanoscience + Engineering, 2015, San Diego, California, United States

A model for traumatic brain injury using laser induced shock waves

A. Selfridge[a], D. Preece[b], V. Gomez[a], L.Z. Shi[a], M.W. Berns[a,c]

[a] University of California, San Diego, Department of Bioengineering, 9500 Gilman Drive, La Jolla, California 92093, United States
[b] University of California, San Diego, Department of NanoEngineering, 9500 Gilman Drive La Jolla, California 92093, United States
[c] University of California, Irvine, Beckman Laser Institute, 1002 Health Sciences Road, Irvine, California 92612, United States

ABSTRACT

Traumatic brain injury (TBI) represents a major treatment challenge in both civilian and military medicine; on the cellular level, its mechanisms are poorly understood. As a method to study the dysfunctional repair mechanisms following injury, laser induced shock waves (LIS) are a useful way to create highly precise, well characterized mechanical forces.

We present a simple model for TBI using laser induced shock waves as a model for damage. Our objective is to develop an understanding of the processes responsible for neuronal death, the ways in which we can manipulate these processes to improve cell survival and repair, and the importance of these processes at different levels of biological organization.

The physics of shock wave creation has been modeled and can be used to calculate forces acting on individual neurons. By ensuring that the impulse is in the same regime as that occurring in practical TBI, the LIS model can ensure that in vitro conditions and damage are similar to those experienced in TBI. This model will allow for the study of the biochemical response of neurons to mechanical stresses, and can be combined with microfluidic systems for cell growth in order to better isolate areas of damage.

Keywords: Laser Induced Shock Wave, Traumatic Brain Injury, Neuron, Actin, Wavelet Decomposition, Cell Surgery, Biophotonics

1. INTRODUCTION

This study demonstrates that the responses of neuron growth cones to shock wave induced damage are quantitatively similar to responses to other laser induced damage, in particular laser sub-axotomy. Additionally, we explore the cytoskeletal dynamics of neurons in response to shock waves, the relationship of these dynamics to different forms of damage, and the possible relevance to TBI.

1.1 Background

The effects of brain injury on cellular processes have been assessed to different extents at both the cellular and organismal level. Models of these two levels are incomplete, however, and bridging the gap is not simple with traditional models of traumatic brain injury. Animal experimentation and clinical research in many ways do not separate the relevant physiological responses to brain injury, although it is easy to recreate the forces responsible for traumatic brain injury[1]. In vitro experiments, conversely, simplify the model to a point where individual pathways are easily probed. This simplification, however, comes at the cost of less reliable

Optical Trapping and Optical Micromanipulation XII, edited by Kishan Dholakia, Gabriel C. Spalding
Proc. of Vol. 9548, 95480P · © 2015 SPIE · CCC code: 0277-786X/15/$18 · doi: 10.1117/12.2189724

damage models[2]. Using various novel computational and optical tools, we have begun to study the response of in vitro cultures of hippocampal neurons to impulses similar to those seen in traumatic brain injury.

Irradiation of a fluid with a high energy, short pulsed laser microbeam initially causes photo-ionization, yielding free electrons, in turn allowing for inverse Bremsstrahlung absorption and avalanche ionization depending on the availability of free electrons. The result of these ionization events is ultimately the formation of a plasma at the laser focus which, due to collision of high energy electrons with surrounding molecules, has high temperature and pressure[3]. As this plasma expands, creating a bubble within the liquid, a shock wave is created which extends up to several hundred microns in diameter. Shock wave pressure can either be measured directly using a hydrophone or calculated indirectly based off of the maximum cavitation bubble diameter[3]. Shock wave pressure is ultimately based on the laser pulse length, numerical aperture of the microscope objective, and energy density of the laser beam. As laser power can be controlled using a wave plate and polarizer, it is simple to modulate the pressure of resultant shock waves, allowing for creation of precise forces and impulses (figure 1). Based on the Gilmore model for bubble expansion and collapse, the expected shear profiles for a given laser power were calculated[4]. Using these models, it is possible to tailor the impulse imparted on the cell such that the damage is in the same regime as that of traumatic brain injury.

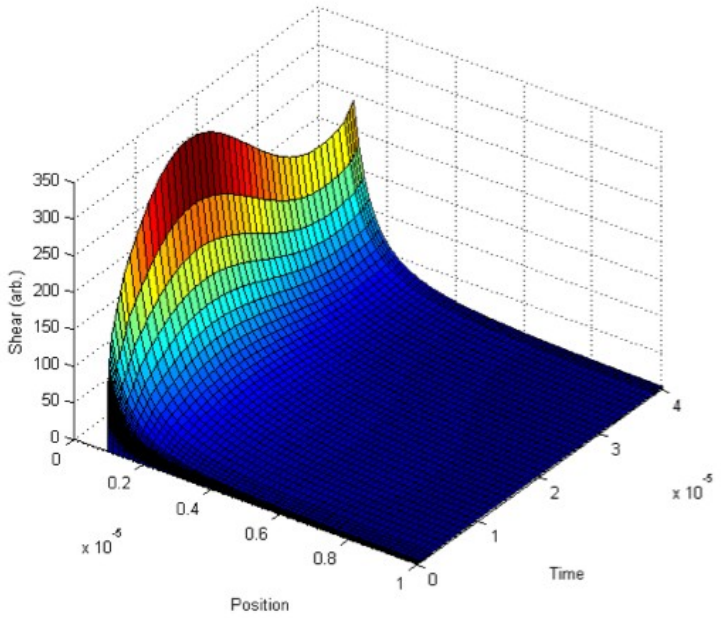

Figure 1: Shear forces calculated by solving of the Gilmore equation for bubble expansion. The graph shows how the shear force changes over time and distance. The bubble rapidly expands and contracts, creating a wave of shear forces. With distance the effects of the wave rapidly diminish.

In order to assess the health and activity of neurons throughout these experiments, an algorithm was developed to quantitatively establish the activity of neuron growth cones in different frequency regimes. Specifically, the algorithm tracks the spatial and temporal localization of high frequency movements, such as the movement of filopodia and lamellipodia, and low frequency movements such as the gradual probing of an axon or migration of the cell body. The algorithm uses a simplified wavelet series decomposition of a stack of images in order to isolate the spatial and temporal information[5]. In the implementation used here, the

information is divided into eight frequency bands through application of an iterative filter bank. The number of frequency bands can be any arbitrary power of two, although greater frequency resolution implies modest increases in computational cost. The filter bank used is comprised of iterative averaging and subtraction operations, which separate frequency bands without the need for large matrix multiplication operations.

1.2 Experiments

Cultures of hippocampal cells were prepared following dissection from fetal rats, and plated on dishes coated with poly-L-lysine. Cells were grown for three to five days in media containing neurobasal, glutamax, and b27 supplement, as described in [6]. Axons several hundred microns in length with active growth cones were targeted for sub-axotomy, a process by which a laser creates damage without completely transecting the axon. Images were acquired using a 63x objective (NA = 1.4), at ten second intervals for five minutes prior to laser exposure. The damage was followed for up to one hour until the damage response appeared to have concluded. The laser used for sub-axotomy was a 532 nm green picosecond pulsed laser (Spectra Physics, Vanguard). The power used was about 21 mW after the objective. After imaging, the time series were qualitatively sorted into (1) positive responses, where axons showed significant repair response following damage, (2) neutral responses, where the growth cones recovered without significant changes in apparent dynamics, and (3) negative responses, where neurons did not recover from damage. These time series were then quantitatively assessed using the wavelet decomposition algorithm, where a region of interest, generally the growth cone, was selected and the wavelet coefficients for each frequency band measured[7].

In shock wave experiments, hippocampal cells were cultured under the same conditions as cutting experiments for three to five days before experimentation. Experiments were imaged using a 40x objective (NA = 1.3) in order to increase the effective field of view and the observable radius of damage of the shock wave. The laser used to create shock waves was a 532 nm green laser with 2 ns pulses (Coherent, Flare). Time series were acquired at ten second intervals for five minutes prior to damage, and for as long as the damage response persisted, up to one hour. The time series were both qualitatively and quantitatively assessed, first manually using ImageJ and later automatically using the described wavelet series decomposition. The relationship between the qualitative response and the dynamics of the wavelet coefficients was used to verify the utility of the algorithm and revisit the relationship posited in the sub-axotomy experiments where negative responses show sharp decreases in wavelet signal magnitude. Using the quantitative measures of neuronal response to both shock wave and ablative damage, the similarities and differences of the two damage models could be identified and analyzed.

In order to establish the parameters relevant to neuronal response to shock wave damage, laser power and positioning were varied, creating a range of different damage conditions. Ideally, the strength of the shock wave is sufficient to elicit a transient change in the neuronal structure without causing cell lysis. Changing laser power had the greatest effect near the threshold for cavitation, since slight decreases in power also decrease the probability of bubble formation. Increasing power appeared to extend the range of damage and cell lysis, and as such laser power was kept to a minimum, but still above the cavitation threshold (about 90μW after the objective). The height of the focal point was positioned ten microns above the surface of the sample in order to ensure that cavitation occurred in bulk, rather than on a boundary layer, where the established models do not necessarily hold[4,8]. The lateral distance necessary to elicit transient responses from neurons was found to be approximately 100 microns. Within this range, cells appeared to lyse, and outside of the range little change in cellular morphology was apparent.

Once neurons could be damaged reliably, the characteristic frequency response of the growth cones was measured using the aforementioned wavelet series decomposition. Using the positive and negative response rates found by wavelet decomposition, the repair mechanisms responsible for recovery following shock wave and sub-axotomy were compared.

Finally, in order to compare the different cytoskeletal dynamics responsible for the shock wave and sub-axotomy repair response mechanisms, neurons were infected with a virus containing LifeAct red fluorescent protein (RFP) plasmid, which codes for a fluorescent protein which binds to existing actin. Expressing neurons were subjected to similar shock wave forces. Both phase and fluorescence images were acquired in order to monitor both the cytoskeletal dynamics and to ensure that the cell remained intact.

2. RESULTS

2.1 Sub-axotomy studies

Growth cone response to damage was qualitatively scored based on the cell's recovery to a baseline of activity established before damage. Cells were grouped into a positive response category if activity appeared to increase following damage, a neutral category if recovery proceeded without noticeable change in activity, and a negative category if activity permanently decreased following damage. The same data were then independently analyzed using the wavelet decomposition algorithm. Growth cones with qualitatively negative responses following sub-axotomy generally also had significant decreases in the magnitude of the wavelet coefficients across all frequency bands. In support of the utility of the wavelet algorithm, all ce1ls which had permanent decreases in wavelet activity of more than 75 percent were independently categorized as having negative damage responses. All cells with less than 75 percent decrease in activity were independently categorized as having neutral or positive responses. Based on this correlation, the dynamics of the wavelet coefficients were judged to be a meaningful indicator of the overall health and activity of the growth cone[7]. The algorithm was later applied to the measurement and classification of growth cone responses to shock wave damage. Similar dynamics were observed in response to shock waves, when neurons which had qualitatively negative response to damage also had overall drops in wavelet coefficients across all frequency bands.

In addition to the quantitative characterization of the growth cone repair mechanism, other characteristics were observed which shed light onto neural damage response mechanisms. Specifically, it was seen that growth cones are capable of sensing and sending filopodial extensions towards a sub-axotomy site on its own axon (figure 2). This behavior was first seen in [9], where growth cones turned towards damage sites on both their own damaged axon or nearby axons which had been damaged. In most cases the turning of the growth cone tended to have a positive effect on the outcome of the repair response[9]. Such responses raise the question of what the damaged axon releases to attract nearby growth cones, how growth cones sense and respond to the chemical gradient, and how interaction of the growth cone with the damage site contributes to the recovery process.

Finally, in order to further characterize the cytoskeletal dynamics of the recovery process, axons were fixed and stained for actin and tubulin at different time points following damage. Based on this staining, actin appeared to accumulate at damage sites, especially in axons exhibiting strong recovery responses. This finding is consistent with the observation that growth cones tend to shuttle material towards damage sites along their own axon, due to the abundance of actin rich structures throughout the growth cone. Additionally, tubulin appears to vacate damage sites along the axon for a sustained period of time before recovering along the axon as the recovery process finishes[7].

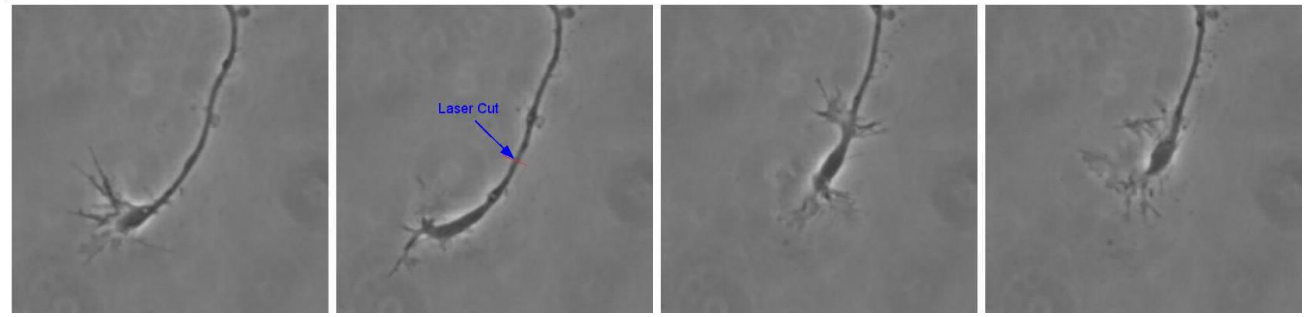

Figure 2: Response of a growth cone to laser ablation. The first panel shows a healthy, active growth cone. The second panel shows the initial response to ablation, indicated by the arrow. The third panel shows a retraction of the growth cone, as well as movement of material from the growth cone distally towards the damage site, presumably as part of the repair mechanism. Finally, the fourth panel shows the recovered growth cone. This growth cone would be qualitatively categorized as a positive damage response. The sequence of four images represents a total elapsed time of 30 minutes.

2.2 Shock wave studies

Similar to the responses observed following sub-axotomy, one typical response of growth cones to shock wave damage is temporary retraction and collapse of the growth cone. In about half of all cases, the growth cone reappears with filopodial and lamellipodial activity similar to that seen before damage. In the remaining half of cases, the growth cone remains inactive and does not recover. Quantitatively, the latter of these two cases is similar to that seen in cutting experiments, where negative response is associated with an approximately 75 percent reduction in wavelet magnitude. The distinction of positive and negative response categories is supported by distinct wavelet dynamics. Positive responses see a return to the baseline wavelet magnitude established before damage, while negative responses see an enduring 75 percent decrease in wavelet magnitude (Figure 3).

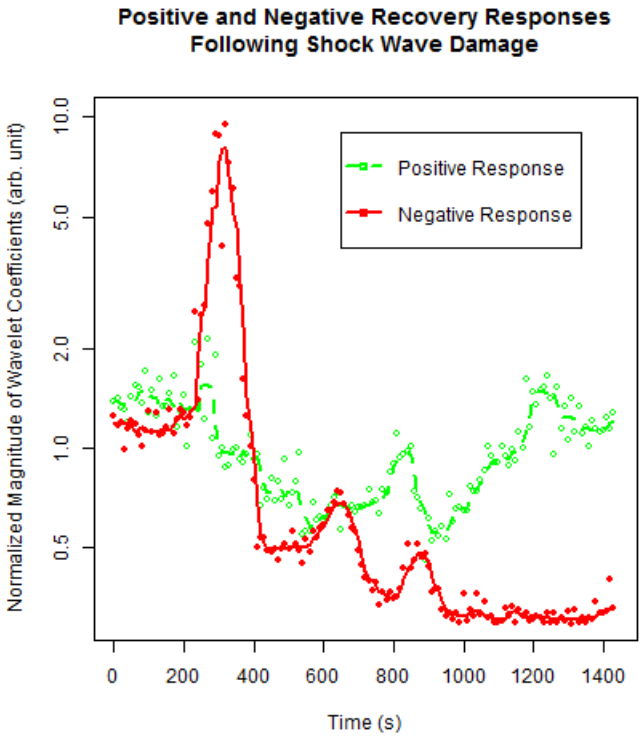

Figure 3: Frequency response of two growth cones in response to shock wave damage. The line shows the median filtered time trace, while the points are the raw frequency data. Both sets are normalized to the mean value. Shock wave occurs at 300 seconds, with a power of about 100μW after the objective and about 100μm from the cell of interest. The green trace shows a typical cell which recovers from shock wave damage, while the red trace shows a cell which does not recover from damage. The sharp peak in the red trace following shock wave is due to a slight shift in focus and a small movement of the stage, both of which appear in the wavelet domain as high energy oscillations.

Experiments using neurons transfected with an actin binding fluorescent protein further elucidated the cytoskeletal dynamics of damage repair mechanisms. Neurons tended to exhibit an outward movement of actin in response to shock wave damage, beginning in the cell body and moving towards the dendrites and axon. This outward flow of fluorescence was quantified using a custom optical flow algorithm that tracked the time of maximum fluorescent intensity at each point in the cell, based on an optical flow algorithm used to quantify cardiac action potential propagation[10]. The algorithm first corrected for photobleaching throughout the time series by maintaining a constant average pixel value across the image area: net changes in fluorescence within neurons were assumed to be small compared to the changes across the whole image which occurred due to photobleaching. The time series was processed and the frame with the greatest pixel value at each location within the image was recorded. Based on this array, various flow characteristics were established and measured, such as direction, magnitude, and velocity of flow.

Cells with qualitatively visible optical flow tended to have early peak fluorescence times near the center of the cell, and late peak fluorescence times at the edges of the cell, implying a movement of actin from the center of the cell body out towards the periphery. These measurements are shown in figure 4A and C, where dark areas (blue) describe areas of the cell with high fluorescent intensity shortly after shock wave. Mid-range colors (cyan and green)

indicate slightly later times of peak fluorescent intensity, followed by light colors (yellow) for the latest fluorescent peaks. The color gradients in figure 4C indicate that actin fluorescence moved outwards towards the dendrites and axons as a response to shock wave damage. The significance of these flow measurements was verified using Jasp, an actin stabilizer, to prevent the movement of actin following damage[11]. As expected, after the addition of Jasp the gradient smooths and becomes less pronounced around the cell, indicating that actin is less free to rearrange itself (Figure 4B, D). The lack of contrast in figure 4D indicates the absence of actin flow due to stabilization of the cell. White areas at the center of the cell indicate areas where the maximum fluorescence occurred before shock wave creation. These areas were removed from analysis.

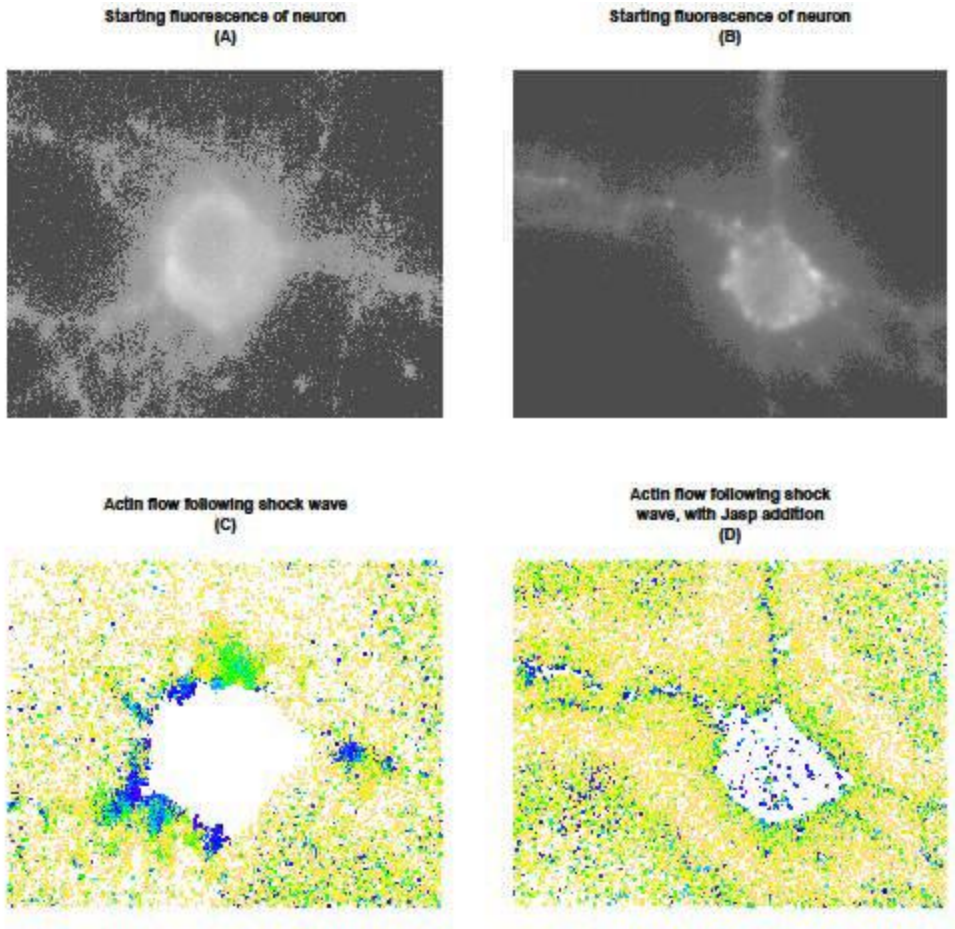

Figure 4: Effect of Jasp on actin flow following shock wave damage. Jasp, an actin stabilizer, inhibits polymerization and depolymerization of actin. (A) and (B) show the initial fluorescence of the cell, with applied threshold to improve contrast. Color gradients in (C) and (D) represent flow of actin. Dark colors (blue) in (C) indicate that the maximum fluorescent intensity occur early after the creation of shock wave. Cyan and green indicate that fluorescence peaked at a point near the middle of the time series. Lighter colors (yellow) indicate that the maximum fluorescent intensity occur longer after shock wave creation, at the end of the time series. High contrast color gradients in (C) indicate outward flow of actin. The lack of color contrast in (D) indicates minimal flow of actin. The slight gradient surrounding the cell body in (D) is likely due to the correction for photobleaching, which causes increases in noise around the cell.

The outward flow of actin and the effect of Jasp were further quantified by averaging pixel values radially, moving outwards from the center of the cell. At each radius, the maximum time point of the peak in fluorescence was recorded. The slope of the resulting vector represents a lower limit for the propagation velocity of the actin wave (figure 5). The green trace in figure 5 is an average of 9 control trials where cells were exposed to LIS without any chemical treatment. The red trace is an average of trials where cells were treated with Jasp and subsequently exposed to LIS. A number of distinctions between the two traces are apparent, particularly the slope, the y-intercept, and the radius at which they reach a maximum value. Cells without Jasp tended to have earlier wave creation (decreased y-intercept) and a greater maximum wave radius, but also had slower outward transport of actin following damage (greater slope).

One potential cause for error in the analysis of actin propagation is the time point at which Jasp was added. The incubation time for each neuron after addition of Jasp varied from about 10 minutes to over an hour. As a result, the extent to which the actin was able to interact with the Jasp was not constant across all cells. Many individual cells showed no gradient at all after the addition of Jasp, while others had gradients similar to the control cells. Regardless of these inconsistencies, however, there exists a significant difference between the rate of outward propagation of actin in cells treated with Jasp and those which were untreated upon damage. The rate of propagation of the actin wave in cells which had not been treated with Jasp was about half that of cells which had been treated.

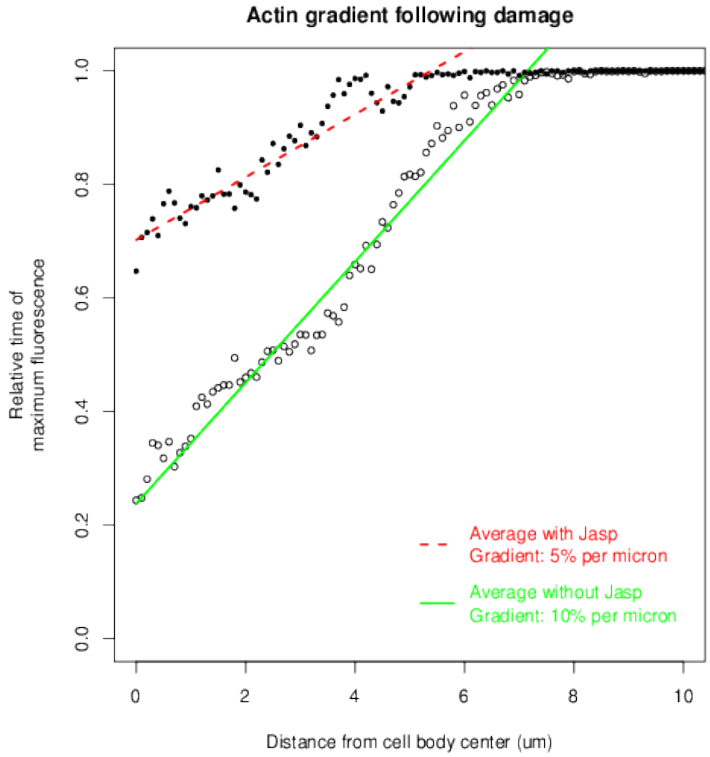

Figure 5: Actin flow gradient following LIS damage, and the effect of Jasp on gradient. The slope of the line is indicative of the steepness of the color gradient in figure 2. Color gradient was measured in 9 cells exposed to shock wave and 9 cells treated with Jasp then exposed to shock wave (n_{totoal} = 18). Values were averaged to produce the two traces above. Larger radii reach peak fluorescence later in the time series, while areas near the center of the cell body tended to peak earlier. Addition of Jasp stabilizes the actin and causes a significant delay in wave onset time and ultimate radius of the wave.

3. DISCUSSION

The similarity between the rates of response of ablative and shock wave damage imply the possibility that the two phenomena may be linked, although further experiments using inhibitors blocking upstream molecules would be necessary. Additionally, the cytoskeletal restructuring in both cases may imply a similar damage response mechanism, despite any superficial differences between the two processes.

A number of programmatic changes could facilitate more accurate flow measurements and better fluorescent data analysis. The correction for photobleaching is currently one step in the analysis which may produce artifacts in the flow measurements. As it currently exists, the correction applies a single fractional change across the whole image. Photobleaching, however, proceeds at an exponential rate proportional to the starting fluorescence. Areas of higher fluorescence bleach faster than areas of low fluorescence, while the implementation used here assumes all areas of the cell bleach at the same rate[12]. Additionally there is, in many images, a slight halo surrounding fluorescent objects which changes in intensity based on both nearby fluorescence and focal plane. The combination of these factors is most likely the cause of the gradient seen in figure 2B. Minimizing artifacts resulting from the correction process and optimizing image contrast will further improve the flow measurements and better demonstrate the cytoskeletal response to shock wave.

A number of explanations are possible of why shock wave damage may cause outward movement of actin. It still remains to be determined, however, whether the cytoskeletal rearrangement is an active process or a passive one. If the process is active, the outward flow could be related to the movement of actin observed in ablative experiments, where actin was shuttled towards a damage site. In the same way that the damaged area of the axon required material in order to facilitate remodeling and recovery, the dendrites and axon may require cytoskeletal components in order to recover following global shock wave damage. Actin shuttled outwards could be responsible for the formation of new focal adhesions necessary for securing neuronal connections with both the environment and other cells, or could be necessary for supporting the cytoskeleton in other ways. Alternatively, rather than active redirection of cytoskeletal material, the outward movement of actin could simply be a result of mechanical shearing of the cytoskeleton within the cell body, resulting in small fragments diffusing to areas in the periphery of cell. While in many ways less biochemically complex, such shearing would provide important insight into the ways that neurons respond to different force regimes.

4. CONCLUSION

4.1 Analysis of damage model

The laser shock wave model appears to be a viable in vitro model for traumatic brain injury. Growth cone dynamics following shock wave damage are similar to those seen after sub-axotomy, although the cytoskeletal dynamics suggest that the global nature of shock waves incites a different response from localized damage.

A similar approach to that described here was shown in [13], where well-characterized shock waves served as a damage model for high throughput assessment of mechanotransduction. Such versatility in implementation underscores the utility of LIS as a method of creating forces within a known regime. In combination with a microfluidic system to control the growth of

positioning of neurons, the LIS model could be a useful tool for conducting high throughput screening of pathways and molecules relevant to TBI. Additionally, combination of optical tools with modern imaging technology such as FRET biosensors allows for quantification of functionally relevant information, such as flux through intracellular pathways and activation of specific proteins[14, 15]. This combination of tools will promote a holistic understanding of the cellular mechanisms responsible for TBI.

4.2 Future goals

The primary goal of future research into neuronal response to LIS damage is to establish a causal relationship between the recovery mechanisms to different types of damage. One major obstacle to this goal is the difficulty of maintaining healthy, active growth cones, especially following LifeAct RFP infection. Through out sub-axotomyand shock wave experiments, neurons were seen to be most active at three days following plating[7]. After infection, however, approximately three days were necessary for the cells to express sufficient protein for imaging. In addition, the infection process appeared to stress the neurons, reducing the ultimate activity. As a result, most of the growth cones in experiments where LifeAct RFP was used were less active than those seen in experiments where no infection was necessary. Addressing such procedural issues will be a significant step towards uncovering the mechanism by which neurons respond to damage, and will expedite experiments requiting direct measurement of actin dynamics.

Various quantitative aspect of the analysis must be improved as well, and the extent of the quantification must be increased. The frequency response of growth cones to shock wave damage must be better cataloged to establish distinct relationships differentiating between the moderate and poor recovery groups. In sub-axotomy experiments, the moderate and poor recovery groups were seen to have a threshold of 75 percent decrease in activity between the first thirty frames and the final thirty frames[7]. Based on the observed dynamics of growth cones following shock wave damage, it is possible that the same frequency dynamics would hold despite the different damage mechanisms. Such data will be useful for establishing the relationship between shock wave and ablative damage, and will allow for more accurate comparisons between the two models.

5. ACKNOWLEDGMENTS

This work was supported by grants from the Beckman Laser Institute Foundation, and from the Air Force Office of Scientific Research under FA9550-14-1-0034.

6. REFERENCES

[1] Ziebell, J. & Morganti-Kossmann, M. “Involvement of pro- and anti-inflammatory cytokines and chemokines in the pathophysiology of traumatic brain injury”, Neurotherapeutics 7, 22-30 (2010).

[2] Morrison, B., Elkin, B., Dollé, J. & Yarmush, M. “In Vitro Models of Traumatic Brain Injury”, Annu Rev Biomed Eng. 13, 91-126 (2011).

[3] Lauterborn, W. & Vogel, A. [Bubble Dynamics and Shock Waves], Springer Berlin Heidelberg, Berlin, 67-103 (2013).

[4] Gilmore, F. R. “The growth or collapse of a spherical bubble in a viscous compressible liquid”, (1952).

[5] Kilmer, W. “A Friendly Guide To Wavelets”, Proc IEEE 86, 2387-2387 (1998).

[6] Wan, J. et al. “Endophilin B1 as a novel regulator of nerve growth factor/ TrkA trafficking and neurite outgrowth”, J. Neurosci. 28, 9002–9012 (2008)

[7] Selfridge, A. et al. “Rat embryonic hippocampus and induced pluripotent stem cell derived cultured neurons recover from laser-induced subaxotomy”, Neurophotonics 2, 015006 (2015).

[8] Hellman, A., Rau, K., Yoon, H. & Venugopalan, V. “Biophysical Response to Pulsed Laser Microbeam-Induced Cell Lysis and Molecular Delivery”, J Biophoton 1, 24-35 (2008).

[9] Wu, T. et al. “Neuronal growth cones respond to laser-induced axonal damage”, J R Soc Interface 9, 535–547 (2012).

[10] Laughner, J. I., Ng, F. S., Sulkin, M. S., Arthur, R. M. & Efimov, I. R. “Processing and analysis of cardiac optical mapping data obtained with potentiometric dyes”, Am J Physiol Heart Circ Physiol 303, H753–H765 (2012).

[11] Bi, A. et al. “Myosin II regulates actin rearrangement-related structural synaptic plasticity during conditioned taste aversion memory extinction”, Brain Struct Funct 220, 813-825 (2013).

[12] Hodgson, L., Nalbant, P., Shen, F. & Hahn, K. “Imaging and Photobleach Correction of Mero - CBD, Sensor of Endogenous Cdc42 Activation”, Methods Enzymol 406, 140-156 (2006).

[13] Compton, J. L., Luo, J. C., Ma, H., Botvinick, E. & Venugopalan, V. “High-throughput optical screening of cellular mechanotransduction”, Nat Photon 8, 710–715 (2014).

[14] Gomez-Godinez, V. et al. “Laser-induced shockwave paired with FRET: a method to study cell signaling”, Microsc Res Tech 78, 195–199 (2015).

[15] Wang, Y. et al. “Visualizing the mechanical activation of Src”, Nature 434, 1040–1045 (2005).